A proteomic approach to the identification of heterogeneous nuclear ribonucleoproteins as a new family of poly(ADP-ribose)-binding proteins

Jean-Philippe GAGNÉ*, Joanna M. HUNTER*, Benoît LABRECQUE†, Benoît CHABOT† and Guy G. POIRIER*[1]

*Health and Environment Unit, Laval University Medical Research Center, Centre hospitalier universitaire de Québec (CHUQ), Faculty of Medicine, Laval University, 2705, Boulevard Laurier, Ste-Foy, Québec, Canada G1V 4G2, and †Department of Microbiology and Infectiology, Faculty of Medicine, Sherbrooke University, 3001, North 12th Avenue, Fleurimont, Québec, Canada J1H 5N4

A new class of poly(ADP-ribose) (pADPr)-binding proteins, heterogeneous nuclear ribonucleoproteins (hnRNPs), has been identified by a proteomic approach using matrix-assisted laser-desorption–ionization time-of-flight ('MALDI-TOF') MS. Liquid-phase isoelectric focusing with a Rotofor® cell (Bio-Rad) allowed pre-fractionation of proteins extracted from HeLa cells. Rotofor® protein fractions were further separated by SDS/PAGE and then transferred to a PVDF membrane. pADPr-binding proteins were analysed by autoradiography of the protein blot after incubation with ^{32}P-labelled automodified pADPr polymerase-1 (PARP-1). Peptide mass fingerprinting of selected bands identified the most abundant pADPr-binding proteins as hnRNPs, a family of proteins that bind pre-mRNA into functional complexes involved in mRNA maturation and transport to the cytoplasm. Sequence homology database searching against a previously reported pADPr-binding sequence motif revealed that the hnRNPs contain a putative pADPr-binding sequence pattern [Pleschke, Kleczkowska, Strohm and Althaus (2000) J. Biol. Chem. **275**, 40974–40980]. pADPr-binding assays performed with synthetic peptides by the dot-blot technique and with nitrocellulose-transferred recombinant hnRNPs confirmed the pADPr-binding protein identification and the specificity of the interaction. These results could establish a link between increased levels of pADPr in DNA damaged cells and the modified protein expression pattern resulting from altered mRNA trafficking.

Key words: heterogeneous nuclear ribonucleoprotein (hnRNP), peptide mass fingerprinting, poly(ADP-ribose) (pADPr), proteomic.

INTRODUCTION

Poly(ADP-ribosyl)ation is a unique post-synthetic modification catalysed by the growing poly(ADP-ribose) (pADPr) polymerase (PARP) family of enzymes in response to DNA-damaging agents [1,2]. Using NAD^+ as a substrate, PARPs catalyse the formation of pADPr with heterogeneous branched chain lengths of up to 200 units *in vitro* [3]. Some of these enzymes, such as PARP-1 and PARP-2, are localized in the nucleus and some, such as PARP-4 and PARP-5, are located in the cytoplasm, but pADPr synthesis takes place mainly in the cell nucleus [3]. Recently, it has been shown that PARP-1 activation is required for translocation of apoptosis-inducing factor ('AIF') from the mitochondria to the nucleus and that PARP-1-dependent cell death is caspase-independent [4]. Also, post-translational poly(ADP-ribosyl)ation of an oscillator component has been proposed to contribute to setting the period length of the *Arabidopsis thaliana* (thale cress) central oscillator [5].

More than 30 nuclear substrates of PARPs have been identified [6]. However, the main acceptor of pADPr is PARP-1 itself, a phenomenon known as 'PARP-1 automodification' [7]. In view of the tremendous negative charge and size of pADPr, poly(ADP-ribosyl)ation of proteins likely has a major impact on protein structure and function.

In the present paper we report a proteomic approach to identify some proteins that bind to pADPr. The most abundant of these pADPr-binding proteins are predominantly heterogeneous nuclear ribonucleoproteins (hnRNPs), a large set of proteins that bind mRNA in the cell nucleus. Although hnRNPs presumably have several different functions, these are not yet all well characterized for each member of the hnRNP family. It has been proposed that hnRNPs help package the pre-mRNA into functional complexes [8]. For example, several hnRNPs are associated with the spliceosome complex [9]. In addition to RNA binding, some hnRNPs are known to bind single-stranded, duplex and triplex DNA [10]. hnRNPs are multifunctional proteins that can influence gene expression through many cellular processes. For example, interaction between hnRNP A1 and inhibitory κBα ('IκBα') is required for maximal activation of nuclear factor κB ('NF-κB')-dependent transcription [11]. There is also considerable evidence that suggests a role for some hnRNPs in the export of mRNA from the nucleus to the cytoplasm [12–14]. The recent finding of telomere-bound hnRNPs suggests that hnRNPs may be involved in the regulation of telomere length [15].

The functions of conserved domains of hnRNP A1 and other hnRNPs have been extensively studied. hnRNP A1 is a 320-amino-acid protein containing two copies of an RNA recognition motif (RRM) at the N-terminus, known as the UP1 domain, and a C-terminal glycine-rich domain (CT) that comprises an M9 nuclear localization signal (NLS) involved in bidirectional nuclear–cytoplasmic transport [16] (Figure 1). RRMs are common and

Abbreviations used: CCD, charge-coupled device; CT, C-terminal glycine-rich domain; DHBB, dihydroxyboryl-Bio-Rex; DTT, dithiothreitol; GST, glutathione S-transferase; HCCA, α-cyano-4-hydroxycinnamic acid; hnRNP, heterogeneous nuclear ribonucleoprotein; MALDI-TOF MS, matrix-assisted laser-desorption–ionization time-of-flight MS; NLS, nuclear localization signal; pADPr, poly(ADP-ribose); PARP, poly(ADP-ribose) polymerase; RO60, ribonucleoprotein 60; RRM, RNA recognition motif; TFA, trifluoroacetic acid.

[1] To whom correspondence should be addressed (e-mail guy.poirier@crchul.ulaval.ca).

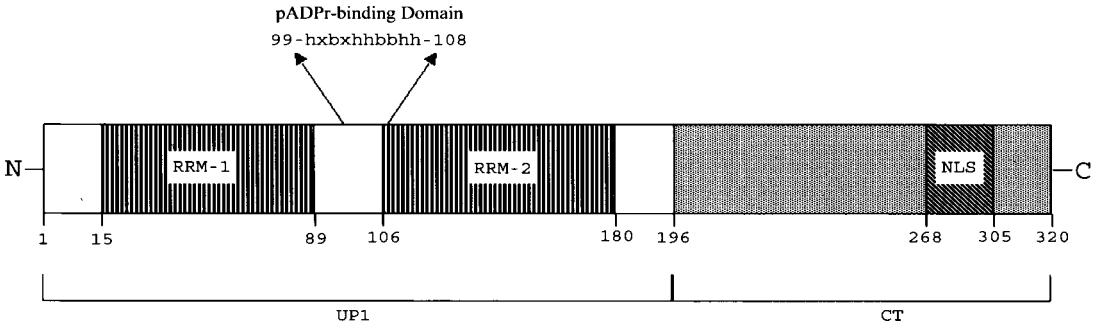

Figure 1 Structure of human hnRNP A1 conserved domains

Arrows indicate the putative consensus pADPr-binding domain. Numbers refer to the amino acid positions from the initiation codon. The positions of RRM and NLS are those specified by Vitali et al. [41] and Izaurralde et al. [16] respectively. The UP1 and CT domains are also indicated below the structure.

evolutionary conserved RNA-binding modules. The two RRMs of hnRNP A1 are closely related, but have distinct functions in regulating pre-mRNA processing. The UP1 and C-terminal domains of hnRNP A1 can independently bind nucleic acids, although this binding is substantially weaker than that observed with intact hnRNP A1 protein [17]. Both the UP1 and the C-terminal domains of hnRNP A1 are required in alternative splicing of mRNA [18].

Recent reports have also suggested the implication of hnRNPs during apoptosis. The cleavage of hnRNP A1 by caspase-3 identified hnRNPs as apoptosis-associated proteins in human Burkitt lymphoma cell line [19]. Subcellular proteome analysis and differential protein expression of apoptotic cells has been very informative regarding hnRNP processing resulting from apoptotic events in the cell [19,20]. Little is known about the physiological significance of the involvement of hnRNPs in apoptosis, but translocation and cleavage of several other hnRNPs have been identified [21].

In the present study we have shown that hnRNPs which bind to pADPr contain a consensus sequence that is responsible for the specific binding and that pADPr binding is a characteristic distinct from RNA binding. The implications of these interactions in mRNA maturation and translocation will be discussed.

MATERIALS AND METHODS

HeLa cell sample preparation

The human cervical adenocarcinoma cell line HeLa-S3 was cultured in suspension (air/CO_2, 19:1; 37 °C) in Eagle's minimal essential medium (S-MEM; Sigma) containing 10 % (v/v) fetal-bovine serum, 100 units/ml penicillin and 100 μg/ml streptomycin. Cell growth was produced in a sterile culture cell spinner. Cell pellets containing 2.6×10^8 cells were washed twice with sterile Hepes buffer and stored at −80 °C. They were then resuspended in 15 ml of the Rotofor® isoelectric-focusing (IEF) buffer [0.2 % Triton X-100/5 M urea/2 M thiourea/2 % CHAPS/2 % Bio-Lytes pH 3–10 (Bio-Rad)/protease-inhibitor cocktail (according to Boehringer's instructions)]. The cell extract was vortex mixed for 5 min to achieve complete cell disruption and protein solubilization, then sonicated at 20 kHz with an amplitude value of 3 for 1 min with a 550 Sonic Dismembrator sonicator (Fisher Scientific). The cell extract was centrifuged at 15000 ***g*** for 15 min to remove extraneous cellular debris. The volume of the cell-protein-extract supernatant was then adjusted to 18 ml with the Rotofor® buffer.

Liquid-phase IEF

A mini Rotofor® preparative cell (Bio-Rad) was used to separate proteins in the liquid phase according to their pI. The solubilized cell pellet was loaded into the Rotofor® focusing chamber without further treatment. A constant power of 10 W was applied to the system, which was cooled to 10 °C with a water circulator. The initial voltage of 450 V reached a plateau of 1800 V after approx. 4 h of focusing time. A total of 20 fractions were collected, and their pH values measured with a microelectrode. Each of the Rotofor® fractions were analysed on 1.5 mm-thick SDS/10 %-(w/v)-polyacrylamide gels, which were silver-stained as described by Mortz et al. [22].

pADPr-binding protein identification

Even-numbered Rotofor® fractions were separated by SDS/10 %-PAGE. Proteins were transferred on to a 0.45 μm-thick PVDF membrane (Bio-Rad) overnight at a constant voltage of 30 V in a system cooled to 4 °C. The membrane was incubated for 1 h at room temperature with gentle agitation in TBS-T [10 mM Tris/HCl (pH 8.0)/150 mM NaCl/0.1 % Tween-20], containing 250 nM of either ^{32}P-labelled automodified PARP-1 or free ^{32}P-labelled pADPr. It was then washed with the TBS-T buffer until no radioactivity could be detected. The membrane was subsequently air-dried and subjected to autoradiography on Bio-Max (Kodak) films.

^{32}P-labelled automodified PARP-1 synthesis

^{32}P-labelled automodified PARP-1 was synthesized essentially as described by Ménard and Poirier [23]. In a total reaction volume of 900 μl [100 mM Tris/HCl (pH 8.0)/10 mM $MgCl_2$/8 mM dithiothreitol (DTT)/10 % (v/v) glycerol/calf thymus activated DNA (23 μg)/1 mM NAD^+], 75 μCi of [^{32}P]NAD^+ was added. Ethanol was added to this preparation dropwise at 10 % (v/v) final concentration, with constant mixing, and the reaction mixture was incubated for 3 min at 30 °C. The reaction was started by adding 20 units [24] of PARP-1 purified up to the

DNA–cellulose step (600 units/mg of protein) as described by Zahradka and Ebisuzaki [24]. After 30 min at 30 °C, during which time the enzyme was modified by covalent linkage of pADPr chains to its automodification domain, 100 μl of 3 M sodium acetate, pH 5.2, and 700 μl of propan-2-ol were added as described by Brochu et al. [25]. The reaction mixture was kept on ice for 30 min and then centrifuged at 10000 ***g*** for 10 min at 4 °C. The pellet was washed twice with ice-cold 80 % (v/v) ethanol and resuspended in 900 μl of TE buffer [10 mM Tris/HCl (pH 8.0)/1 mM EDTA]. Calculating from the radioactivity count before and after synthesis, the percentage of NAD^+ incorporation was 16 %. The final pADPr concentration was 162 μM.

^{32}P-labelled free pADPr

Following ^{32}P-labelled automodified PARP-1 synthesis, the protein-bound pADPr was hydrolysed by incubation with 1 ml of 1 M KOH and 50 mM EDTA solution at 60 °C. After 1 h, 9 ml of AAGE9 buffer [250 mM ammonium acetate (pH 9.0)/6 M guanidine/10 mM EDTA] was added and the pH was adjusted to 9.0 with 4 M HCl. The free pADPr was isolated on a dihydroxyboryl Bio-Rex (DHBB) resin synthesized as described by Shah et al. [26]. A 0.5 ml portion of DHBB was packed into a 10 ml Econo column (Bio-Rad) and washed with 5 ml of water and 10 ml of AAGE9 buffer. The sample was loaded on the DHBB, the flow-through was reloaded, and the resin was washed with 20 ml of AAGE9 buffer, followed by 10 ml of 1 M ammonium acetate, pH 9.0. The free ^{32}P-labelled pADPr was eluted with five portions of 0.5 ml of water at 37 °C. Fractions 2 and 3, corresponding to the peak of radioactivity, were pooled.

Identification of pADPr-binding proteins by peptide mass fingerprinting

Prior to the protein extraction and identification on the matrix-assisted laser-desorption–ionization time-of-flight (MALDI-TOF) mass spectrometer, the ^{32}P-labelled pADPr was removed from the proteins by incubating the PVDF membrane for 30 min in a 0.1 M NaOH solution containing 20 mM EDTA. Bands excised from the PVDF membrane were rinsed with de-ionized water and cut into pieces of approx.imately 1×1 mm^2. To each band, 100 μl of 25 mM ammonium bicarbonate in 10 % acetonitrile was added. Proteins in the PVDF membrane pieces were reduced by adding 3 μl of 45 mM DTT and incubating for 20 min at 37 °C. Alkylation was accomplished by adding 3 μl of 100 mM iodoacetamide and incubating the mixture in the dark for 20 min. This buffer was then removed, and 100 μl of 25 mM ammonium bicarbonate in 10 % acetonitrile and 0.1 % octyl β-D-glycopyranoside was added. The samples were incubated at 37 °C for 20–24 h with 5 μl of 0.1 mg/ml trypsin (Promega Sequencing Grade Modified Trypsin).

An α-cyano-4-hydroxycinnamic acid (HCCA) matrix solution was prepared as a saturated solution in 50 % acetonitrile and 0.1 % trifluoroacetic acid (TFA). A 1 μl aliquot of the digestion solution was pipetted directly on to a dried 0.8 μl spot of HCCA on the sample plate. The spot was allowed to dry and then another 1 μl was deposited. Finally, the crystallized sample spot was washed twice with 2 μl of 0.1 % TFA. An Applied Biosystems Voyager-DE™ PRO Biospectrometry™ Workstation was used to acquire positive-ion mass spectra. Data were collected in reflectron mode at an acceleration voltage of 20 kV and an extraction delay time of 200 ns. Spectra were internally calibrated using the [*M* (the molecular ion) + H]$^+$ peaks at 842.502 and 2211.097 Da resulting from trypsin autoproteolysis.

Peptide masses measured by MALDI-TOF MS were submitted to PeptIdent (ExPASy Molecular Biology server) for searching against the SwissProt database or to ProFound (Proteometrics) for searching the NCBI (National Center for Biotechnology Information, U.S. National Library of Medicine Bethesda, MD, U.S.A.) non-redundant protein database. The mass-tolerance parameter for matching monoisotopic [M + H]$^+$ ion masses was set at 30 p.p.m. Protein molecular masses were constrained to $\pm$100 % of the measured molecular mass, and pI values were not restricted (0–14 pH units). A maximum of 1 missed trypsin cleavage was allowed in the search. Results were evaluated and prioritized based on sequence coverage and matching of the theoretical to the measured molecular mass and pI.

Dot-blot analysis of the pADPr-binding domain

The amino acid sequences of histone H4, ribonucleoprotein 60 (RO60), hnRNP A1 and hnRNP A2 were searched for sequence homology with the pADPr-binding sequence motif given by Pleschke et al. [27]. Searching for this binding pattern was accomplished using the ScanProsite tool on the ExPASy Molecular Biology server. Peptides corresponding to the putative pADPr-binding domain of these proteins as well as alanine-substituted peptide sequences from the original hnRNP A2 were synthesized using fluoren-9-ylmethoxycarbonyl ('Fmoc') technology on an Applied Biosystems 433A peptide synthesizer. For the dot-blot analysis, the following peptides were used:

histone H4: KRHRKVLRDNIQGITKPAIRRLARR

RO60: FKKDLKESMKCGMWGRALRKA

hnRNP A1: REDSQRPGAHLTVKKIFVGGIK

hnRNP A2: REESGKPGAHVTVKKLFVGGIK

hnRNP A2 substitution #1:

AAAAAAPGAHVTVKKLFVGGIK

hnRNP A2 substitution #2:

REESGKPGAAVTVAALFVGGIA

hnRNP A2 substitution #3:

REESGKPAAHATAKKAFVGGIK

hnRNP A2 substitution #4:

REESGKPGAHVTVKKAAAAAAK

negative control 1: CHRPLMRNQKSRDSS

negative control 2: HEGVYIEPEARGRLC

The dot-blot was performed essentially as described by Panzeter et al. [28]. Peptides were dissolved in TBS-T and 2 μg of each peptide was spotted on to a 0.05 μm nitrocellulose membrane (Schleicher und Schüll). The membrane was air-dried, rinsed three times with TBS-T and incubated for 1 h at room temperature (22 °C) with gentle agitation in TBS-T containing 250 nM ^{32}P-labelled automodified PARP-1 or free ^{32}P-labelled pADPr. It was then washed with TBS-T buffer until no radioactivity could be detected. The membrane was subsequently air-dried and subjected to autoradiography on Bio-Max (Kodak) films.

Immunological detection of pADPr-binding peptides

The TBS-T washing of the membrane was followed by a 1 h incubation at room temperature with TBS-T containing 250 nM free non-radioactive pADPr. The membrane was rinsed three

times with TBS-T and incubated in PBS-MT (PBS buffer containing 5% non-fat dried milk and 0.1% Tween-20) for 1 h. The anti-pADPr antiserum 96-10 (1:10000 in PBS-MT) [29] was applied overnight with gentle agitation at room temperature. The membrane was washed several times with PBS-MT and incubated for 30 min with a secondary anti-rabbit antibody (1:2500 in PBS-MT) conjugated with peroxidase (Jackson ImmunoResearch Laboratories). The membrane was washed and revealed using the Renaissance chemiluminescence kit (NEN Life Sciences, now PerkinElmer Life Sciences). One dot-blot control membrane was stained with SYPRO™ Ruby Red stain (Molecular Probes) in order to evaluate the uniformity of peptide retention on the membrane, as displayed by the integrated density value of the fluorescence intensity on a UV-based charge-coupled-device (CCD) camera (Alpha Innotech Corporation, San Leandro, CA, U.S.A.).

SYPRO™ Ruby Red protein blot stain

The nitrocellulose membrane was fixed in 10% (v/v) methanol and 7% (v/v) acetic acid for 15 min. The membrane was rinsed three times with water and covered for 30 min, with gentle agitation, with SYPRO™ Ruby Protein blot stain. The blot was rinsed for 15 min with water and revealed using a fluorescence-based CCD imaging system (Alpha Innotech Corporation).

Expression and purification of hnRNP conserved domains

Plasmids pGEX-A1 and pGEX-A2 were constructed by inserting the mouse hnRNP A1 and hnRNP A2 cDNAs [30] into the *Eco*RI site of pGEX-2T. The hnRNP UP1 fragment was produced as described in LaBranche et al. [31] and was inserted into the *Eco*RI site of pGEX-2T. pGEX-hnRNP A1ΔRRM2 was produced by the deletion of the *Bgl*II–*Msc*I fragment and contains a linker element. hnRNP A1ΔRRM2 therefore lacks amino acids 107–171, but contains instead amino acids Ile-Ser-Ser-Ser. The fragment hnRNP A1-CT containing amino acids 194–319 was produced by PCR and cloned in pGEX-2T.

All recombinant glutathione S-transferase (GST)–hnRNP fusion proteins were expressed in *Escherichia coli* BL21. Bacteria were grown for 2–3 h at 37 °C until reaching an attenuance (D_{600}) between 0.5 and 1.0. Induction with 100 μM isopropyl 1-thio-β-D-galactopyranoside ('IPTG') was performed for 4 h. Cells were washed with cold Rec-Buffer [50 mM piperazine/HCl (pH 9.8)/500 mM NaCl/1 mM DTT/1 mM EDTA/0.5 mM PMSF/1 mM benzamidine/bacitracin (20 mg/ml)] and resuspended with 10 ml of Rec-Buffer/100 ml of culture. Lysozyme (0.4 mg/ml) was added 30 min before sonication. Cells were sonicated for 15 s and left on ice for 30 s. The cycle was repeated another three times. Triton X-100 was added to a final concentration of 1%, and the mixture was incubated for 30 min at room temperature on a rotating device. After a 10 min centrifugation at 12000 ***g*** at 4 °C, 600 ml of GSH–Sephadex (from a 50% slurry in Rec-Buffer) was added to the supernatant. The mixture was incubated for 30 min at 4 °C, then centrifuged 20 s at 500 ***g*** and washed four times with Rec-Buffer containing 0.1% Triton X-100. GST-proteins were eluted with 300 ml of a buffer comprising 20 mM GSH, 200 mM piperazine, pH 9.8, 1 mM DTT, 1 mM EDTA and 500 mM NaCl. Eluted material was dialysed in Buffer D [20 mM Hepes/KOH (pH 7.9)/100 mM KCl/20% (v/v) glycerol/0.2 mM EDTA/1 mM DTT/0.5 mM PMSF]. A 1 μg portion each of recombinant hnRNPs, core histones and GST–protein was separated by electrophoresis on 0.75-mm-thick SDS/12% -polyacrylamide gel. The proteins were transferred on to a 0.05-μm-thick nitrocellulose membrane (Schleicher und Schüll). A constant voltage (125 V) was applied for 1 h to the system, which was cooled to 4 °C. Membranes were washed three times with TBS-T before incubation with ^{32}P-labelled automodified PARP-1. Competition assays using RNA and NAD^+ were also performed in order to evaluate specificity of pADPr binding to hnRNPs. A 100-fold excess of yeast RNA (Ambion) or NAD^+ (Boehringer Mannheim) over pADPr was added to the incubation buffer. Again, the membranes were washed until no radioactivity could be detected in theTBS-T buffer. On occasions, membranes were washed under high-stringency conditions (1 M NaCl in TBS-T). The membranes were air-dried and subjected to autoradiography on Bio-Max (Kodak) films.

RESULTS

Identification of pADPr-binding proteins

Liquid-phase IEF followed by SDS/PAGE was used to fractionate proteins from a HeLa-cell protein extract. Prefractionation by liquid-phase IEF decreases considerably the sample complexity prior to SDS/PAGE. Moreover, preparative IEF permits much higher protein load than does a conventional two-dimensional gel, ranging up to the milligrams of protein. Twenty Rotofor® fractions of HeLa-cell proteins were collected over an almost linear pH range from 2 to 10 (Figure 2). Rotofor® fractions analysed by SDS/PAGE (Figure 3) illustrate that most of the proteins do not focus in only one pH fraction, but rather spread over two or more pH fractions with a clear enrichment pattern in some of these fractions. The goal of this two-step separation is to minimize the number of co-migrating proteins. Although MALDI-TOF MS can deal with multiple protein identification within a band, it is desirable to obtain a single protein per band.

After transfer of the PAGE-separated proteins to a PVDF membrane and exposure to ^{32}P-labelled automodified PARP-1, autoradiography reveals the putative pADPr-binding proteins (Figure 4). On comparison of the very different patterns obtained from silver-stained gel and autoradiography obtained with ^{32}P-labelled automodified PARP-1, one can observe that cellular proteins do not bind the pADPr in proportion to their abundance. As expected, the pADPr-binding patterns obtained from SDS/

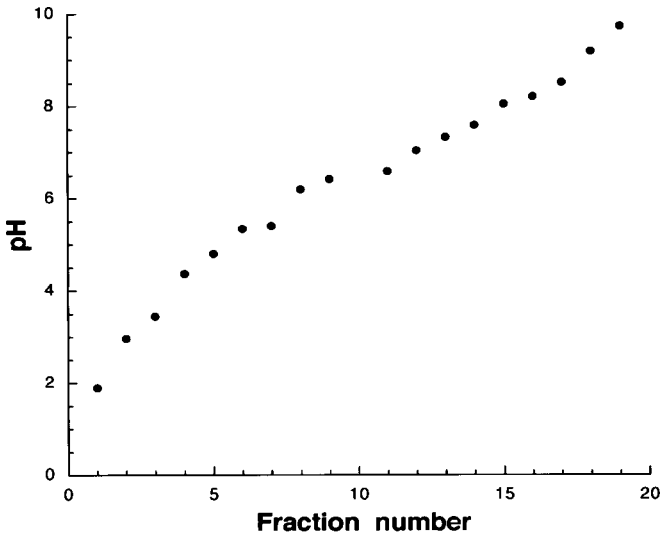

Figure 2 pH evaluation of Rotofor® fractions harvested from a pH 3–10 electrofocusing chamber

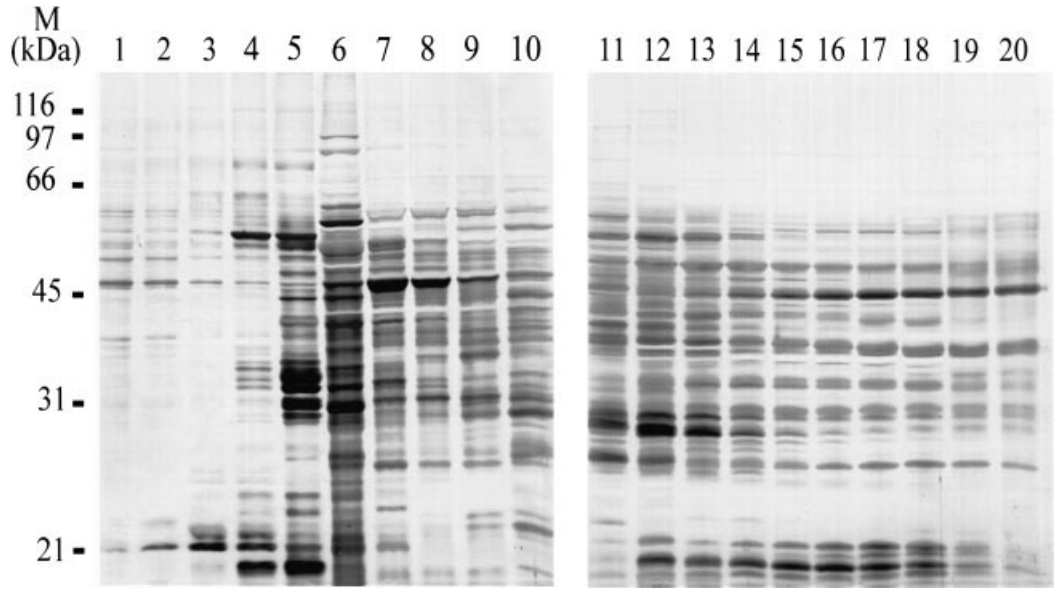

Figure 3 Silver-stained SDS/PAGE of Rotofor® fractions

The fraction numbers are indicated over each lane. M is molecular mass.

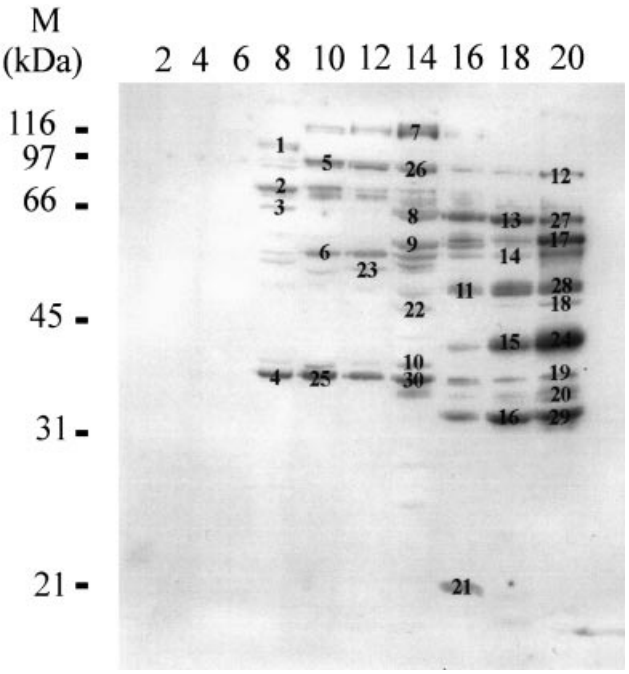

Figure 4 Analysis of pADPr-binding proteins

Even-numbered fractions harvested from the Rotofor® cell were transferred on to PVDF membrane. Incubation with ^{32}P-automodified PARP-1 or free [^{32}P]pADPr followed by autoradiography reveals a binding-protein pattern. Numbered bands were excised for identification by peptide mass fingerprinting. Rotofor® fraction numbers are indicated over each lane. M is molecular mass.

PAGE-separated Rotofor® fractions using either automodified PARP-1 or free pADPr are identical (results not shown). This observation indicates that the interaction is a protein–pADPr contact rather than a protein–protein interaction. Considering that most of the cellular pADPr is protein-bound and that PARP-1 is the most important pADPr acceptor, the use of automodified PARP-1 is more likely to be representative of the interaction.

A total of 30 of the higher-intensity bands were cut from the membrane and analysed by peptide mass fingerprinting after trypsin digestion. The mass spectrum shown in Figure 5 is a tryptic digest from the band number 29 (see Figure 4) in which hnRNP A2/B1 and annexin II co-migrated. In this particular band, the use of recombinant hnRNP A2 showed that hnRNP A2 is actually the pADPr-binding protein, even if the relative intensity of hnRNP A2 peptides is considerably lower compared with annexin II. There were 15 tryptic peptides identified from hnRNP A2/B1 and eight peptides from annexin II. MALDI-TOF MS identification reveals many hnRNPs as pADPr-binding proteins (hnRNP A2/B1, hnRNP C1/C2, hnRNP E1, hnRNP G, hnRNP H, hnRNP K and hnRNP M) as well as previously reported pADPr-binding proteins such as lamins and histones (Table 1). Note that the majority of these proteins have a basic pI. The identity of the proteins in other bands will be the subject of further study. In general, no identifications were obtained from bands having a molecular mass higher than 90 kDa, probably because the higher-molecular-mass proteins are not efficiently transferred to the membrane. Most of the pADPr-binding proteins were localized in a single protein band, but some hnRNPs co-migrated with other proteins.

Characterization of pADPr binding on synthetic peptides by dot-blot analysis

In order to characterize further this pADPr affinity, we attempted to localize the pADPr-binding site of hnRNPs on the basis of a previously reported pADPr-binding consensus sequence [27] (see Figure 6). This consensus pattern consists of approx. 20 amino acids: a N-terminal cluster rich in basic residues (lysine/arginine) and a C-terminal region containing alternating hydrophobic and basic amino acids (Figure 6A). A search with the PATTINPROT

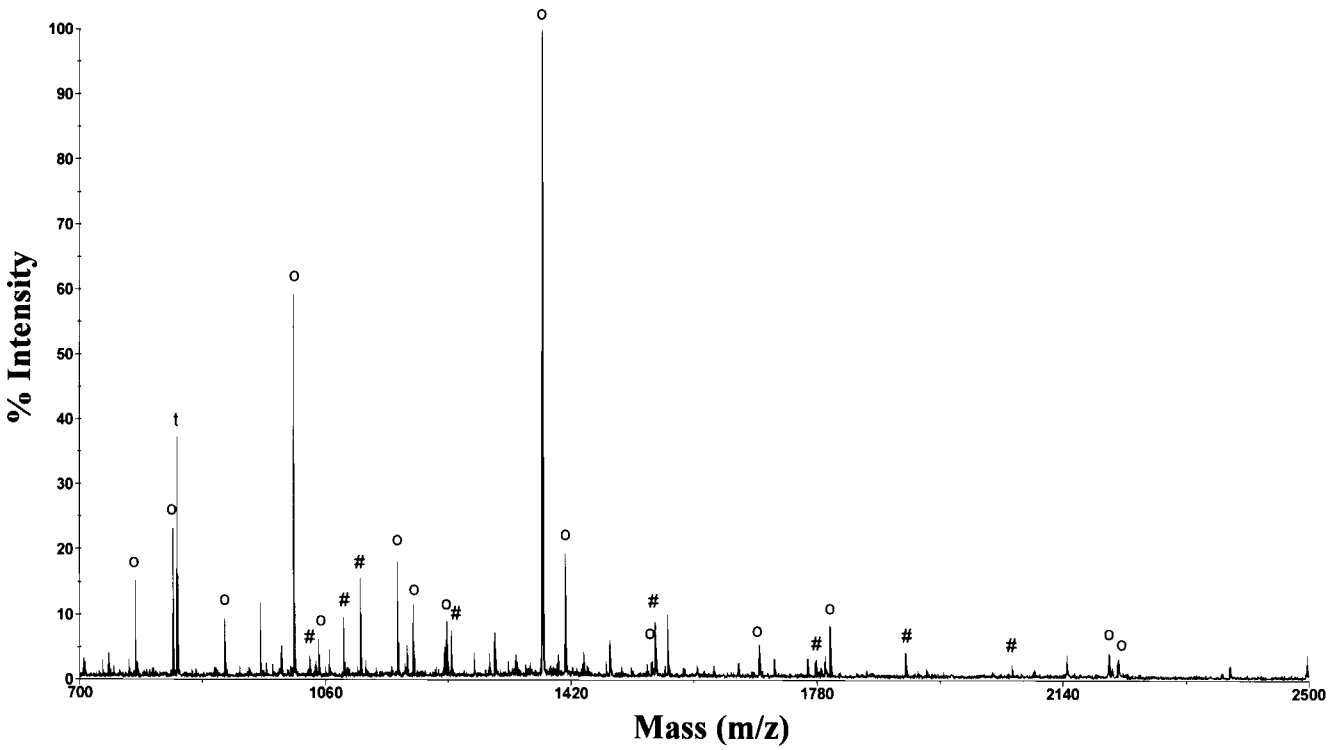

Figure 5 Tryptic-peptide mass map of the proteins in band number 29

Peptides from two proteins, hnRNP A2/B1 (#) and annexin II (°), were identified in this band. Trypsin autolysis products (t) are also labelled.

Table 1 pADPr-binding proteins from a HeLa-cell extract identified by peptide mass fingerprinting

Bands were excised from the membrane shown in Figure 4.

				pI/molecular mass (Da)	
Band no.	Tentative protein identification	SwissProt or GeneBank® accession no.	Sequence coverage (%)	Theoretical	Estimated
4	hnRNP C1/C2 (2 isoforms)	P07910	20	5.11/33 299; 5.10/31 966	6/39 000
6	hnRNP K (2 isoforms)	Q07244	19	5.39/50 976; 5.19/51 028	6.5/57 000
8	Lamin A/C	P02545	40	6.57/74 139	8/66 000
9	Lamin A/C (second isoform)	P02545	30	6.4/65 135	8/60 000
16	hnRNP A2/B1 (isoform) and Annexin II	P22626; P07355	37; 31	8.67/36 006; 7.56/38 473	9/35 000
20	hnRNP A2/B1	P22626	19	8.97/37 430	10/38 000
21	Histone H1C	P16402	22	11.02/22 219	8.5/20 000
22	hnRNP H	P31943	17	5.9/49 229	8/50 000
24	hnRNP G (RNA-binding motif protein) and phosphoglycerate kinase 1	P38159 (11421425); P00558 (6456828)	40; 37	10.02/42 404; 8.3/44 597	10/42 000
25	hnRNP C1/C2 (2 isoforms)	P07910	19	5.11/33 299; 5.10/31 966	6.5/39 000
27	hnRNP M (2 isoforms)	P52272	31	8.94/77 470; 9.03/73 575	10/66 000
29	hnRNP A2/B1(2 isoforms) and annexin II	P22626; P07355	46; 25	8.97/37 430 or 8.67/36 006; 7.56/38 473	9/35 000
30	hnRNP C1/C2 (2 isoforms) and hnRNP E1 (α-CP1)	P07910; Q15365 (2134737)	25; 20	5.11/33 299 (5.10/31 966); 6.66/37 526	8/39 000

tool on the NPS@ server (Network Protein Sequence @nalysis, http://npsa-pbil.ibcp.fr/) [32] revealed that all of the identified hnRNPs may contain such a pADPr-binding site, it being borne in mind that the pADPr-binding domain does not contain invariant amino acids at a given position within the consensus. Multiple sequence alignment of related hnRNPs with the consensus sequence reveals a closely matching pattern (Figure 6B).

To verify whether the putative pADPr-binding domain of hnRNPs does indeed bind to pADPr, a pADPr-binding dot-blot analysis was performed on synthetic peptides that display the consensus sequence. The Western blot shown in Figure 7(B) clearly demonstrates that the putative pADPr-binding domain of histone H4, RO60, hnRNP A1 and hnRNP A2 mediates pADPr binding. The use of different approaches to characterize the pADPr-binding affinity of dot-blotted synthetic peptides results in approximately the same pattern of binding affinities. Using either radiolabelled automodified PARP-1 and free pADPr or the immunological detection of pADPr with the 96-10 antibody

A

```
hnRNP A0                          REDSARPGAHAKVKKLFVGGLK
hnRNP A1                          REDSQRPGAHLTVKKIFVGGIK
hnRNP A2                          REESGKPGAHVTVKKLFVGGIK

Consensus                         bxxxxbxhxbx hbbhhhhhhb
pADPr-binding consensus     [xxxxK/Rxxx]xhxbxhhbbhhbxxxx

hnRNP A2 Substitution #1          AAAAAAPGAHVTVKKLFVGGIK
hnRNP A2 Substitution #2          REESGKPGAAVTVAALFVGGIA
hnRNP A2 Substitution #3          REESGKPAAHATAKKAFVGGIK
hnRNP A2 Substitution #4          REESGKPGAHVTVKKAAAAAAK
```

B

Identified hnRNPs	Pattern site	Similarity (%)
hnRNP A2/B1	106-**GAHVTVKKLF**-115	93
hnRNP C1/C2	92-R**GKAGVKRSA**-101	86
hnRNP E1	25-**VGSIIGKKGE**-34	71
hnRNP G	118-**GTRGPPSRGG**-127	78
hnRNP H	210-**YDRPGAGRGY**-219	79
hnRNP K	261-**FDRMPPGRGG**-270	78
hnRNP M	212-D**YKVGWKKL**K-221	86

Figure 6 (A) Sequence alignment of the putative pADPr-binding sequence for closely related hnRNPs corresponding to the dot-blot peptide synthesis and (B) putative pADPr-binding site and similarity with the consensus sequence for all hnRNPs identified by peptide mass fingerprinting

(**A**) The basic amino acids (b) are lysine, arginine and histidine, and the hydrophobic amino acids (h) are alanine, cysteine, glycine, valine, isoleucine, leucine, methionine, phenylalanine, tyrosine and tryptophan. Positions indicated by 'x' can be any amino acid. Positions in **bold** are consensus amino acids common to both sequences. The sequence of the hnRNP A2 peptides modified by replacement with alanine is aligned with the pADPr-binding consensus sequence. Substituted amino acid positions are underscored. (**B**) The given similarity percentages are those calculated from the PATTINPROT algorithm [32].

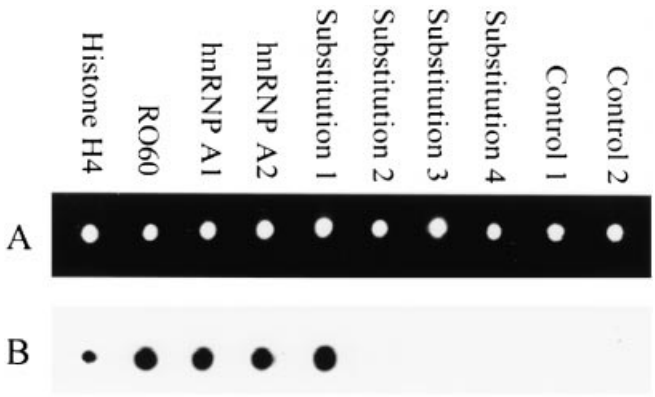

Figure 7 pADPr-binding dot-blot analysis

Different peptides that comprise the putative pADPr-binding site (see the text) were blotted on to nitrocellulose membrane. (**A**) SYPRO Ruby Red blot stain. (**B**) Immunological detection of pADPr-binding peptides in the presence of 250 nM automodified PARP-1. Detection was accomplished by using the anti-pADPr rabbit polyclonal antibody 96-10 in a Western-blot assay.

did not modify the observed pADPr-binding affinity. Moreover, the use of high-stringency buffers (TBS-T with 1 M NaCl) did not abolish pADPr-binding (results not shown). The immunological detection of protein-bound pADPr is presented in Figure 7.

In addition, we have verified by SYPRO Ruby Red blot staining that the quantity of each peptide retained on the membrane was the same (Figure 7A). Uniformity of the peptide retention on the nitrocellulose membrane allows a direct comparison between the pADPr-binding efficiencies of each peptide. To obtain the same amount of each peptide bound to the nitrocellulose membrane, we evaluated the fluorescence intensity of a standardized blot stained with Sypro Ruby Red. The integrated density value of the fluorescence intensity for each of these peptides was approximately the same, indicating an equal amount of peptide retained on the membrane.

It has been proposed that the hydrophobic amino acids in the binding motif are necessary for pADPr binding, whereas the basic residues are less critical [27]. To test this hypothesis, the hnRNP A2 peptide sequence was selectively modified by alanine substitution of all basic and hydrophobic amino acids. The substituted peptides are listed in Figure 6(A). As shown in Figure 7, when the N-terminal tail of the consensus sequence is replaced by alanine (substitution 1), the peptide does not significantly decrease the binding to pADPr. Consequently the consensus could be localized to the hydrophobic/basic region of the consensus without the lysine/arginine-rich cluster at the N-terminus. Replacement by alanine of all the basic residues in the consensus sequence (substitution 2) completely inhibits pADPr binding, as does replacing the hydrophobic residues (substitution 3). Finally, replacement by alanine of the C-terminal residues also abolishes pADPr binding. That the two most hydrophobic residues of the putative pADPr-binding sequence (leucine and phenylalanine) are replaced with residues of much lower hydrophobicity could explain the complete loss of pADPr binding. In contrast with what has been proposed, both interspersed hydrophobic and basic amino acids seem to be important in achieving pADPr binding. Also, preliminary results with random-generated

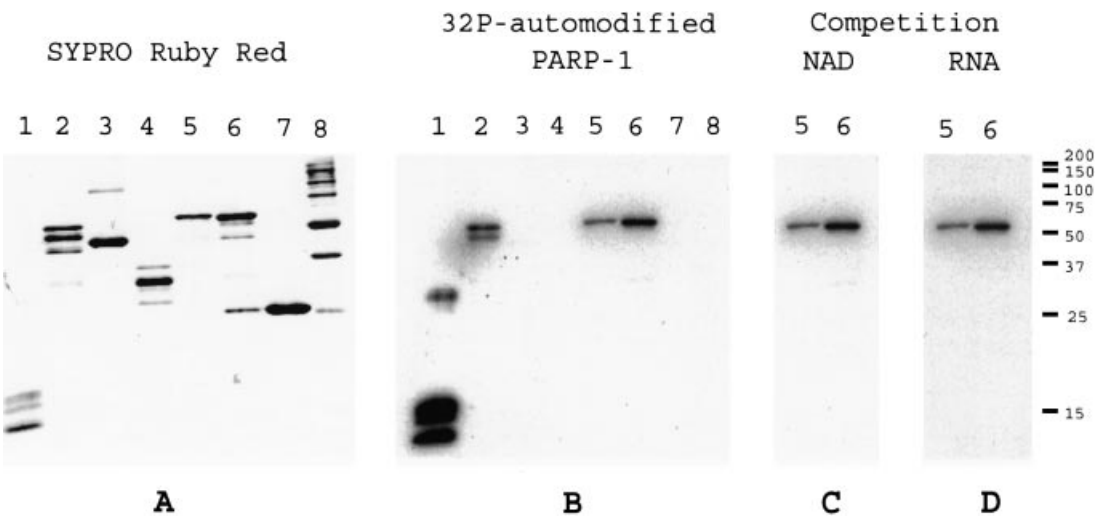

Figure 8 pADPr-binding pattern of the conserved hnRNP domain

Recombinant purified hnRNP protein constructs (1 μg) were separated on SDS/12%-PAGE, followed by transblot on to nitrocellulose membrane. Membranes were stained with SYPRO Ruby Red protein blot stain (**A**), incubated with 250 nM ^{32}P-automodified PARP-1 in TBS-T (**B**), 250 nM ^{32}P-automodified PARP-1 with a 100-fold excess of NAD$^+$ (**C**) or 250 nM ^{32}P-automodified PARP-1 with a 100-fold excess of RNA (**D**). Lanes: 1, core histones; 2, GST–hnRNP A1ΔRRM2; 3, GST–hnRNP A1 UP1 domain; 4, GST–hnRNP A1 C-terminal domain; 5, GST–hnRNP A2 full length; 6, GST–hnRNP A1 full length; 7, GST protein; 8, molecular-mass standards (molecular masses are given in kDa on the extreme right).

hnRNP A1 mutants did not allow us to point out single critical amino acid positions within the pADPr-binding site.

Characterization of pADPr binding on hnRNP conserved domains

Recombinant purified hnRNP–GST hybrid proteins were used in a pADPr-binding assay in order to characterize further the binding specificity of hnRNPs (Figure 8). A SYPRO Ruby Red blot stain of purified hnRNP conserved domains is shown in Figure 8(A). Recombinant hnRNPs constructs migrated at their expected molecular mass, but some proteolysis is apparent. As expected, GST constructs of hnRNP A1 and hnRNP A2 strongly bound pADPr (Figure 8B). Core histones and purified GST were used as positive and negative control samples respectively. Indeed, histones are strong binders of pADPr in this system, while no binding is observed for the GST protein. Specific domains of hnRNP A1 were also expressed as a hybrid protein with GST. No binding is observed for either part of the UP1 or CT domains of hnRNP A1. However, a GST construct exhibiting hnRNP A1 protein with a deletion of the RRM2 does bind to pADPr. This result reveals that RRM2 is not involved in pADPr binding, because the complete deletion of this RRM did not decrease the apparent affinity. However, the UP1 and CT domains constructs failed to bind pADPr. Such a result was expected with the glycine-rich CT domain, as it does not contain the putative pADPr-binding site. Surprisingly, the UP1 domain construct that contains the two intact RRMs and the putative pADPr-binding site did not bind any pADPr. Apparently, the glycine-rich CT domain could be required for adequate position and availability of the pADPr-binding site within the UP1 domain, since pADPr-binding is restored when hnRNP constructs containing both the CT domain and pADPr-binding site are present [full-length hnRNP A1 and hnRNP A1ΔRRM2]. Unfortunately, structural information is not available for the intact hnRNP A1 protein, and therefore the possible structural effect of the CT domain on pADPr-binding is not known.

The unchanged pADPr-binding affinity of the hnRNP A1 lacking a RRM2 sequence is interesting, because it segregates RNA binding from pADPr binding. This observation is also confirmed by competition assays using excess RNA or NAD$^+$ over pADPr (Figures 8B and 8C). Exactly the same binding pattern and intensity was observed, indicating that there is no change in pADPr-binding affinity. These interactions are very specific, because they are observed under physiological or high-stringency conditions (1 M NaCl). Moreover, the inability of competitive RNA or NAD$^+$ to affect the binding efficiency is also a strong indication that pADPr binding to hnRNPs is a specific process.

DISCUSSION

Using a proteomic approach, we have identified a new family of proteins that bind to pADPr, namely hnRNPs. Prasad et al. [33] have previously reported the ADP-ribosylation of hnRNP A1 and hnRNP A2/B1. At that time, it was impossible to determine whether these hnRNPs were modified by single or multiple covalently linked ADP-ribose units. In view of our results it is clear, however, that hnRNPs can establish a strong non-covalent link with pADPr. We demonstrate for the first time that hnRNPs have specific affinity to pADPr resulting from a non-covalent interaction mediated by a consensus motif within the amino acids sequence. Although the function of non-covalent interactions between free pADPr and proteins is poorly understood, it has been demonstrated that non-covalent interactions between the pADPr nuclear proteins such as p53 and histones are very stable and could modify the functional properties of these and other proteins in living cells [34–36]. Therefore, these previous results substantiate our finding that hnRNPs are specific non-covalent pADPr binders.

The interaction between hnRNPs and pADPr could play several cellular functional roles. Given the fact that poly(ADP-

ribosyl)ation is an early response to DNA damage, the affinity of hnRNPs to pADPr, which plays important roles in RNA maturation and translocation, is intriguing. For instance, the interaction of hnRNPs with pADPr could be a mechanism for controlling RNA maturation, because hnRNPs are involved in RNA splicing [8].

PARP-1 translocation to the nucleoplasm during DNA damage and apoptosis [37,38] could affect RNA maturation through the interaction of automodified PARP-1 with hnRNPs. The interaction proposed with PARP-1 is consistent with the nuclear distribution of hnRNPs. The previous finding that hnRNP A1 is specifically cleaved by caspase-3 proteases also supports the link between hnRNPs and apoptosis events [19].

PARP-1 has been shown to be involved in DNA damage signalling through its interaction with p53, p21 and other proteins [39]. Indeed, PARP-$1^{-/-}$ cells are extremely sensitive to γ-irradiation [40]. Part of this signalling mechanism could be the retention of hnRNPs in the nucleus during the peak of pADPr synthesis by PARP-1 in response to DNA-damaging agents. Thus, pADPr synthesis could affect cytoplasmic shuttling during apoptosis and DNA damage. Also, because there is a very large increase of pADPr levels during apoptosis, hnRNP packaging and transport out of the nucleus could be affected by pADPr binding.

We hope that our results will provide important insights into the potential modulation role that pADPr binding to hnRNPs may play in mRNA processing and trafficking into the cell, especially during apoptosis-related cellular events.

This work was supported by the Canadian Institute of Health Research. We thank Isabelle Kelly for peptide synthesis. We also thank Dr Eric Winstall for informative discussions.

REFERENCES

1 Juarez-Salinas, H., Sims, J. L. and Jacobson, M. K. (1979) Poly(ADP-ribose) levels in carcinogen-treated cells. Nature (London) **282**, 740–741

2 Lindahl, T., Satoh, M. S., Poirier, G. G. and Klungland, A. (1995) Post-translational modification of poly(ADP-ribose) polymerase induced by DNA strand breaks. Trends Biochem. Sci. **20**, 405–411

3 D'Amours, D., Desnoyers, S., D'Silva, I. and Poirier, G. G. (1999) Poly(ADP-ribosyl)ation reactions in the regulation of nuclear functions. Biochem. J. **342**, 249–268

4 Yu, S. W., Wang, H., Poitras, M. F., Coombs, C., Bowers, W. J., Federoff, H. J., Poirier, G. G., Dawson, T. M. and Dawson, V. L. (2002) Mediation of poly(ADP-ribose) polymerase-1-dependent cell death by apoptosis-inducing factor. Science **297**, 259–263

5 Panda, S., Poirier, G. G. and Kay, S. A. (2002) tej defines a role for poly(ADP-ribosyl)ation in establishing period length of the *Arabidopsis* circadian oscillator. Dev. Cell **3**, 51–61

6 Althaus, F. R. and Richter, C. (1987) ADP-Ribosylation of Proteins: Enzymology and Biological Significance, Springer-Verlag, Berlin

7 Ogata, N., Ueda, K., Kawaichi, M. and Hayaishi, O. (1981) Poly(ADP-ribose) synthetase, a main acceptor of poly(ADP-ribose) in isolated nuclei. J. Biol. Chem. **256**, 4135–4137

8 Krecic, A. M. and Swanson, M. S. (1999) hnRNP complexes: composition, structure, and function. Curr. Opin. Cell Biol. **11**, 363–371

9 Bennett, M., Pinol-Roma, S., Staknis, D., Dreyfuss, G. and Reed, R. (1992) Differential binding of heterogeneous nuclear ribonucleoproteins to mRNA precursors prior to spliceosome assembly *in vitro*. Mol. Cell. Biol. **12**, 3165–3175

10 Guillonneau, F., Guieysse, A. L., Le Caer, J. P., Rossier, J. and Praseuth, D. (2001) Selection and identification of proteins bound to DNA triple-helical structures by combination of 2D-electrophoresis and MALDI-TOF mass spectrometry. Nucleic Acids Res. **29**, 2427–2436

11 Hay, D. C., Kemp, G. D., Dargemont, C. and Hay, R. T. (2001) Interaction between hnRNPA1 and IκBα is required for maximal activation of NF-κB-dependent transcription. Mol. Cell. Biol. **21**, 3482–3490

12 Michael, W. M., Siomi, H., Choi, M., Pinol-Roma, S., Nakielny, S., Liu, Q. and Dreyfuss, G. (1995) Signal sequences that target nuclear import and nuclear export of pre-mRNA-binding proteins. Cold Spring Harbor Symp. Quant. Biol. **60**, 663–668

13 Michael, W. M., Choi, M. and Dreyfuss, G. (1995) A nuclear export signal in hnRNP A1: a signal-mediated, temperature-dependent nuclear protein export pathway. Cell **83**, 415–422

14 Pinol-Roma, S. and Dreyfuss, G. (1992) Shuttling of pre-mRNA binding proteins between nucleus and cytoplasm. Nature (London) **355**, 730–732

15 Ford, L. P., Wright, W. E. and Shay, J. W. (2002) A model for heterogeneous nuclear ribonucleoproteins in telomere and telomerase regulation. Oncogene **21**, 580–583

16 Izaurralde, E., Jarmolowski, A., Beisel, C., Mattaj, I. W., Dreyfuss, G. and Fischer, U. A. (1997) Role for the M9 transport signal of hnRNP A1 in mRNA nuclear export. J. Cell Biol. **137**, 27–35

17 Casas-Finet, J. R., Smith, Jr, J. D., Kumar, A., Kim, J. G., Wilson, S. H. and Karpel, R. L. (1993) Mammalian heterogeneous ribonucleoprotein A1 and its constituent domains. Nucleic acid interaction, structural stability and self-association. J. Mol. Biol. **229**, 873–889

18 Mayeda, A., Munroe, S. H., Caceres, J. F. and Krainer, A. R. (1994) Function of conserved domains of hnRNP A1 and other hnRNP A/B proteins. EMBO J. **13**, 5483–5495

19 Brockstedt, E., Rickers, A., Kostka, S., Laubersheimer, A., Dorken, B., Wittmann-Liebold, B., Bommert, K. and Otto, A. (1998) Identification of apoptosis-associated proteins in a human Burkitt lymphoma cell line. Cleavage of heterogeneous nuclear ribonucleoprotein A1 by caspase 3. J. Biol. Chem. **273**, 28057–28064

20 Thiede, B., Dimmler, C., Siejak, F. and Rudel, T. (2001) Predominant identification of RNA-binding proteins in Fas-induced apoptosis by proteome analysis. J. Biol. Chem. **276**, 26044–26050

21 Thiede, B., Siejak, F., Dimmler, C. and Rudel, T. (2002) Prediction of translocation and cleavage of heterogeneous ribonuclear proteins and Rho guanine nucleotide dissociation inhibitor 2 during apoptosis by subcellular proteome analysis. Proteomics **2**, 996–1006

22 Mortz, E., Krogh, T. N., Vorum, H. and Gorg, A. (2001) Improved silver staining protocols for high sensitivity protein identification using matrix-assisted laser desorption/ionization-time of flight analysis. Proteomics **1**, 1359–1363

23 Ménard, L. and Poirier, G. G. (1987) Rapid assay of poly(ADP-ribose) glycohydrolase. Biochem. Cell. Biol. **65**, 668–673

24 Zahradka, P. and Ebisuzaki, K. (1984) Poly(ADP-ribose) polymerase is a zinc metalloenzyme. Eur. J. Biochem. **142**, 503–509

25 Brochu, G., Duchaine, C., Thibeault, L., Lagueux, J., Shah, G. M. and Poirier, G. G. (1994) Mode of action of poly(ADP-ribose) glycohydrolase. Biochim. Biophys. Acta **1219**, 342–350

26 Shah, G. M., Poirier, D., Duchaine, C., Brochu, G., Desnoyers, S., Lagueux, J., Verreault, A., Hoflack, J. C., Kirkland, J. B. and Poirier, G. G. (1995) Methods for biochemical study of poly(ADP-ribose) metabolism *in vitro* and *in vivo*. Anal. Biochem. **227**, 1–13

27 Pleschke, J. M., Kleczkowska, H. E., Strohm, M. and Althaus, F. R. (2000) Poly(ADP-ribose) binds to specific domains in DNA damage checkpoint proteins. J. Biol. Chem. **275**, 40974–40980

28 Panzeter, P. L., Zweifel, B., Malanga, M., Waser, S. H., Richard, M. and Althaus, F. R. (1993) Targeting of histone tails by poly(ADP-ribose). J. Biol. Chem. **268**, 17662–17664

29 Affar, E. B., Duriez, P. J., Shah, R. G., Winstall, E., Germain, M., Boucher, C., Bourassa, S., Kirkland, J. B. and Poirier, G. G. (1999) Immunological determination and size characterization of poly(ADP-ribose) synthesized *in vitro* and *in vivo*. Biochim. Biophys. Acta **1428**, 137–146

30 Ben-David, Y., Bani, M. R., Chabot, B., De Koven, A. and Bernstein, A. (1992) Retroviral insertions downstream of the heterogeneous nuclear ribonucleoprotein A1 gene in erythroleukemia cells: evidence that A1 is not essential for cell growth. Mol. Cell. Biol. **12**, 4449–4455

31 LaBranche, H., Dupuis, S., Ben-David, Y., Bani, M. R., Wellinger, R. J. and Chabot, B. (1998) Telomere elongation by hnRNP A1 and a derivative that interacts with telomeric repeats and telomerase. Nat. Genet. **19**, 199–202

32 Combet, C., Blanchet, C., Geourjon, C. and Deleage, G. (2000) NPS@: network protein sequence analysis. Trends Biochem. Sci. **25**, 147–150

33 Prasad, S., Walent, J. and Dritschilo, A. (1994) ADP-ribosylation of heterogeneous ribonucleoproteins in HeLa cells. Biochem. Biophys. Res. Commun. **204**, 772–779

34 Panzeter, P. L., Realini, C. A. and Althaus, F. R. (1992) Noncovalent interactions of poly(adenosine diphosphate ribose) with histones. Biochemistry **31**, 1379–1385

35 Nozaki, T., Masutani, M., Akagawa, T., Sugimura, T. and Esumi, H. (1994) Non-covalent interaction between poly(ADP-ribose) and cellular proteins: an application of a poly(ADP-ribose)–Western blotting method to detect poly(ADP-ribose) binding on protein-blotted filter. Biochem. Biophys. Res. Commun. **198**, 45–51

36 Malanga, M., Pleschke, J. M., Kleczkowska, H. E. and Althaus, F. R. (1998) Poly(ADP-ribose) binds to specific domains of p53 and alters its DNA binding functions. J. Biol. Chem. **273**, 11839–11843
37 Alvarez-Gonzalez, R., Spring, H., Muller, M. and Burkle, A. (1999) Selective loss of poly(ADP-ribose) and the 85-kDa fragment of poly(ADP-ribose) polymerase in nucleoli during alkylation-induced apoptosis of HeLa cells. J. Biol. Chem. **274**, 32122–32126
38 Germain, M., Affar, E. B., D'Amours, D., Dixit, V. M., Salvesen, G. S. and Poirier, G. G. (1999) Cleavage of automodified poly(ADP-ribose) polymerase during apoptosis. Evidence for involvement of caspase-7. J. Biol. Chem. **274**, 28379–28384
39 Wesierska-Gadek, J. and Schmid, G. (2001) Poly(ADP-ribose) polymerase-1 regulates the stability of the wild-type p53 protein. Cell. Mol. Biol. Lett. **6**, 117–140
40 Ménissier de Murcia, J., Niedergang, C., Trucco, C., Ricoul, M., Dutrillaux, B., Mark, M., Oliver, F. J., Masson, M., Dierich, A., LeMeur, M. et al. (1997) Requirement of poly(ADP-ribose) polymerase in recovery from DNA damage in mice and in cells. Proc. Natl. Acad. Sci. U.S.A. **94**, 7303–7307
41 Vitali, J., Ding, J., Jiang, J., Zhang, Y., Krainer, A. R. and Xu, R. M. (2002) Correlated alternative side chain conformations in the RNA-recognition motif of heterogeneous nuclear ribonucleoprotein A1. Nucleic Acids Res. **30**, 1531–1538

Received 25 October 2002/17 December 2002; accepted 8 January 2003
Published as BJ Immediate Publication 8 January 2003, DOI 10.1042/BJ20021675